

Study of Spin-Exchange Collisions in Vapors of Rb⁸⁵, Rb⁸⁷, and Cs¹³³ by Paramagnetic Resonance*†

H. WARREN MOOS‡§ AND RICHARD H. SANDS

Department of Physics, University of Michigan, Ann Arbor, Michigan

(Received 18 December 1963)

The effective spin-dephasing cross sections of Rb⁸⁵, Rb⁸⁷, and Cs¹³³ caused by spin-exchange collisions have been measured using paramagnetic resonance techniques to examine the Zeeman transitions of these alkalis. The collision frequency was determined from the width of the absorption lines and the density of atoms by comparing the intensity of the signal with a CuSO₄·5H₂O crystal in the same cavity. The spin-dephasing cross sections of Rb⁸⁵, Rb⁸⁷, and Cs¹³³ are 2.0, 1.9, and 2.3×10⁻¹⁴ cm². The 70% probable error is ±20%. The relation of these measured dephasing cross sections to the spin-exchange cross sections is discussed. The thermal relaxation times were measured also; it was found that they were best explained by the strong exchange coupling which enhanced a relatively weak relaxation mechanism.

I. INTRODUCTION

WITH the development of optical pumping as a tool for studying many atoms, spin-exchange collisions^{1,2} have received a renewed interest.^{3,4} They enter these experiments both as a source of linewidth and as a means of polarization transfer. This paper is a report of the measurement of spin-exchange dephasing cross sections for rubidium-rubidium and cesium-cesium atomic collisions. The method was a paramagnetic resonance experiment at 9000 Mc/sec. From the width of the absorption spectra the lifetime in a spin state was determined, while the number of alkali atoms was determined by comparing the signal with that of a weighed and oriented copper sulfate (CuSO₄·5H₂O) crystal⁵ located in the same microwave cavity. From the number of alkali atoms per cc and the lifetime, an effective cross section could be computed.

Measurements of the alkali exchange cross sections have been made previously by optical pumping techniques^{4,6}; however, knowing the number of atoms per cc has always been a problem in these experiments.⁷

Moreover, although the techniques described here requires much higher densities than optical pumping, the relation between the lifetime and linewidth is somewhat simpler since other characteristic times do not enter into this experiment. This method of determining a cross section is of interest because of its relatively high accuracy (±20%) and may be used, with only slight changes in technique, to measure similar quantities⁸ in the rest of the alkalis and, in fact, in any atom having a net electronic spin.

We first discuss the effect of spin-exchange collisions and then go on to describe the experimental determination of the linewidth, $1/T_2$, as a function of density. Finally, the measurement of the thermal relaxation times T_1 is discussed and it is shown that the shortness of these measured times may be explained by spin-exchange collisions transferring energy to other pairs of levels which are not interacting with the rf field.

The measured cross sections defined by

$$\sigma_{\text{deph}} = 1/N\bar{v}_{\text{rel}}T_2 \quad (1)$$

are quite large, on the order of 10⁻¹⁴ cm². Estimating effects other than spin exchange which will lead to a dephasing such as dipole-dipole interactions, we find that the largest contributors are distortion of the $AI \cdot S$ hyperfine interaction and interaction with the magnetic moment of the excited p state mixed in during a strong collision. These lead to cross sections of 10⁻¹⁶ cm² to 10⁻¹⁵ cm², which are an order of magnitude below the measured values.

II. SPIN-EXCHANGE COLLISIONS

If two alkali atoms pass sufficiently close, there is a probability that the two electrons will interchange spin coordinates.^{1,2} The physical basis for this is the electrostatic "exchange potentials," which are different for symmetric and antisymmetric combinations of the

* Most of this work is taken from the thesis of one of the authors (HWM) submitted in partial fulfillment of the requirements for the Ph.D. at the University of Michigan.

† Work carried out with the partial support of the U. S. Atomic Energy Commission.

‡ National Science Foundation Cooperative Graduate Fellow during most of this investigation.

§ Present address: Physics Department, Stanford University, Stanford, California.

¹ E. M. Purcell and G. B. Field, *Astrophys. J.* **124**, 542 (1956).

² J. P. Wittke and R. H. Dicke, *Phys. Rev.* **103**, 620 (1956).

See also J. P. Wittke, Ph.D. thesis, Princeton University, 1955 (unpublished).

³ H. G. Dehmelt, F. M. Pipkin, and J. C. Baird, Jr., *Phys. Rev.* **120**, 1279 (1960); W. Holloway, Jr., and R. Novick, *Phys. Rev. Letters* **1**, 367 (1958).

⁴ P. Franken, R. Sands, and J. Hobart, *Phys. Rev. Letters* **1**, 118 (1958); R. Novick, and H. E. Peter, *Phys. Rev. Letters* **1**, 54, 152 (1958).

⁵ L. S. Singer and J. Kommandeur, *J. Chem. Phys.* **34**, 133 (1961). H. Kumagai, I. Hayashi, K. Ono, H. Abe, J. Shimada, and H. Shono, *J. Phys. Soc. Japan* **9**, 376 (1954).

⁶ T. R. Carver, in *The Ann Arbor Conference on Optical Pumping*, edited by P. Franken and R. Sands (The University of Michigan, Ann Arbor, 1959), p. 29.

⁷ A study of the densities in an optical pumping bulb by S. Jarrett has indicated that one may easily be off by as much as a factor of three from the equilibrium vapor pressure. See S. Jarrett, thesis, University of Michigan, 1962 (unpublished).

⁸ For example, spin-exchange cross sections, disorientation cross sections for alkali buffer gas collisions, charge exchange between the alkalis and various organic molecules, etc. For similar measurements in H, see A. F. Hildebrandt, F. B. Booth, and C. A. Barth, *J. Chem. Phys.* **31**, 273 (1959); and R. M. Mayo, *J. Chem. Phys.* **34**, 169 (1961).

atomic orbitals. The two-atom complex is described by mixtures of the two combinations, and under the effect of the exchange potentials one component advances in phase over the other, leading to an interchange of the spin coordinates. This process is much more effective in changing spin orientations than any of those previously mentioned.

In a paramagnetic resonance experiment, the linewidth is described in terms of a characteristic time T_2 . In our case, where the lines are Lorentzian, $1/T_2$ is half the linewidth in radians at half-absorption. At resonance there is a rotating magnetization vector normal to the static magnetic field and the rotating rf field H_1 of the order of $M \sim \chi_0 H_0 \gamma H_1 T_2$, where $\chi_0 H_0$ is the static magnetization corresponding to the large dc field, γH_1 is the rate at which the magnetization vector in the rotating reference frame rotates about H_1 , and $1/T_2$ is the rate at which spins are removed from the rf magnetization vector. This removal may be due either to processes which leave the spins in the rf plane but cause them to scramble phase with respect to the rf field or to thermal relaxation processes which change the orientation of the spins from the rf plane.

Consider the spin exchange of two atoms, the first of which is precessing at the rf frequency about the dc field and which lies along the rf field. After exchange the second atom will, in general, have acquired a spin component along the rf field. Angular momentum is always conserved in such a collision, and therefore the magnetization vector in the rf plane remains unchanged at that instant. However, if the second atom has a nucleus of different m_I orientation so that its spin precesses in the dc field at a rate different from the rf field, it will very quickly lose or gain phase with respect to the rf field, and this component will be removed from the magnetization vector. (The experiment was performed at large magnetic fields and is discussed here in the approximation that the nucleus and electronic spins are only weakly coupled. In the case of Cs^{133} this is not true. Theoretical work is in progress in an attempt to understand this latter case.⁹)

Only half of the spins' angular momenta need be reversed in order to reduce the rotating rf magnetization vector to zero. Furthermore, collisions with atoms of the same m_I do not remove angular momenta from the magnetization vector. Therefore, the measured dephasing cross section is given by

$$\sigma_{\text{deph}} = 2[2I/(2I+1)]\sigma_{\text{ex}}, \quad (2)$$

where σ_{ex} is the collision cross section for *exchange* of spin angular momenta irrespective of the spin states of the atom involved.

In the case of atomic hydrogen,^{1,2} theoretical analysis

⁹ It remains to be shown whether the simple relationship between the dephasing and the spin-exchange cross sections demonstrated to hold at high fields also holds in the intermediate field case. T. Stark of this laboratory is undertaking a study of this question.

indicates that at reasonable temperatures, the only collisions which contribute significantly to the cross section are strong collisions in which the relative phase changes by hundreds of radians. For two atoms approaching each other with an impact parameter such that a strong collision will take place, the probability of an exchange taking place is $\frac{1}{4}$. This can be seen by noting that in only half the collisions will the atoms have oppositely paired spins allowing a strong interaction, and when such collisions do take place the probability of exchange is $\frac{1}{2}$. It then follows from the previous paragraph that, for strong exchange potential controlled collisions, the measured dephasing cross section is equal to half of the geometrical strong interaction cross section [neglecting the $2I/(2I+1)$ factor] as shown by Currin.¹⁰ At present, there is no evidence or calculation on the relative contribution of weak, small phase-change collisions to the spin-exchange cross sections of the alkalis. However, the wave functions of these atoms are quite extensive and van der Waals forces appear to control their spatial motion; it therefore would not be surprising if the strong collision assumption were strictly valid only in the case of hydrogen.^{1,2}

Spin exchange may also assist thermal relaxation by allowing polarization to be transferred from one pair of spin levels to another. Thus, many more atoms may be undergoing thermally relaxing collisions than are absorbing rf photons, and the effective relaxation time is shortened considerably, particularly for the higher spin alkalis. The contribution of this to the linewidth will be discussed in Secs. VIII and IX.

III. SHAPE OF THE LINE

The lines studied here are broadened by random collisions and, for sufficiently low rf field intensities in the cavity, are Lorentzian. The absorption may be described by a susceptibility of the type¹¹

$$\chi'' = \frac{N\mu_{ij}^2}{(2I+1)(2S+1)kT} \frac{\omega_{ij}T_2}{1 + (\omega_{ij} - \omega)^2 T_2^2}, \quad (3)$$

where N is the number of atoms per cc,

$$\mu_{ij} = g\mu_B \langle i | \mathbf{S} \cdot \mathbf{H}_{\text{rf}} | j \rangle / H_{\text{rf}},$$

¹⁰ The reader is referred to the theoretical work by J. D. Currin, Phys. Rev. **126**, 1995 (1962). The important quantity is the effective spin-exchange collision frequency [see Eq. (2.20b)]

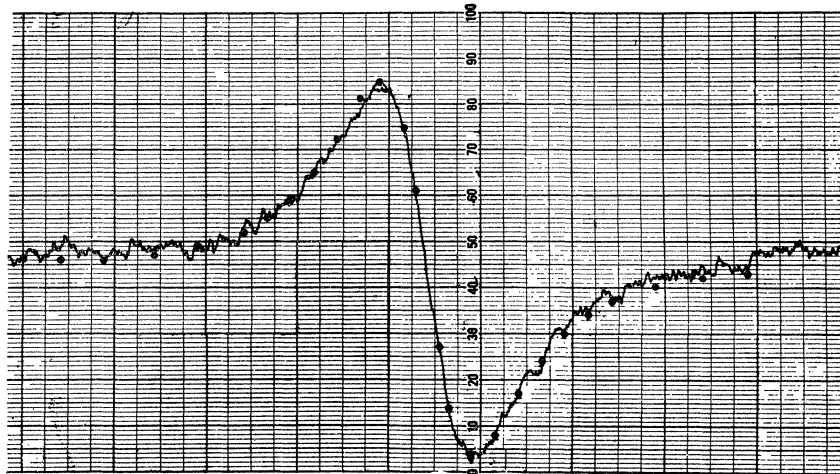
$$q = \lambda N \int \Phi(\Delta) \sin^2(J\Delta/2) d\Delta,$$

where λN is the collision rate, $\Phi(\Delta)$ is the distribution of collision times as a function of Δ . For $J \sim 1$ eV and $\Delta \sim 10^{-12}$ sec, $J\Delta \gg 1$ and the integral becomes $\frac{1}{2}$. Thus one obtains $q = \lambda N/2$. In the case of low q , Currin obtains a Lorentzian line [Eq. (2.28)] with a width in rad/sec of $q(1 - \rho_\alpha)$, where ρ_α is the statistical weight of the α th line, which is in this case, $1/(2I+1)$. Noting that $\lambda N = \nu_{\text{rel}} \sigma_{\text{coll}}$, by use of our Eq. (1), one obtains

$$\sigma_{\text{deph}} = (\sigma_{\text{coll}}/2)[2I/(2I+1)].$$

¹¹ J. H. Van Vleck and V. F. Weisskopf, Rev. Mod. Phys. **17**, 227 (1945); J. P. Lloyd, Ph.D. thesis, Washington University, 1953, Part II (unpublished).

FIG. 1. Alkali line shape compared with a Lorentzian shape.



ω_{ij} is the frequency difference between the two levels of interest in rad/sec, and $(2I+1)(2S+1)$ is the total number of levels resulting from the application of the external magnetic field and the hyperfine structure. This equation is similar to the usual Bloch susceptibilities.¹²

Experimentally, the derivative of the alkali line shape was studied, and when this was compared with the derivative Lorentzian shape (see Fig. 1) agreement was found to be very good.

Copper sulfate¹³ is a somewhat different case. There is a large spin interaction between the very close copper ions. Furthermore, there are two magnetically inequivalent sites for the copper ions which should produce two lines at certain orientations of the crystal in the magnetic field. However, a rapid exchange of electrons among the ions averages out the effects of environment, producing a single, narrowed, nearly Lorentzian-shaped line midway between the expected position of the two.

Lorentzian-shaped lines, however, have an extremely large contribution in the tails of the line. In the case of the alkalis, one would expect the line to be Lorentzian very far out. Atoms have exponentially decaying probabilities of remaining in a state except during the first 10^{-12} sec when they are undergoing a collision. The finite duration of the collision affects the shape only at 10^{12} cycles from the resonance frequency. The copper ion is in a solid with electron magnetic dipoles a lattice distance away. Because of the exchange interaction, the line is narrowed. However, one would not be surprised if the line deviated from the Lorentzian shape in the tails. We find that the $\text{CuSO}_4 \cdot 5\text{H}_2\text{O}$ line agrees with the predicted Lorentzian derivative shape out to more than three linewidths (peak-to-peak line-

width). This agrees with other studies.¹⁴ Using Eq. (3) and making the extreme assumption that the absorption drops to zero at this point (it does not), we calculate that the true intensity, and hence number, would be 20% below that computed from the height and width, if the line is Lorentzian. In this experiment, one knows the number of ions (from the weight of the crystal) and compares the widths and heights of the alkali and copper sulfate signals. This would mean that the measured number of alkali atoms would be 20% too low, and hence, the computed cross sections 20% too high. This correction of 20% is an extreme value, which the true correction is certainly quite a bit below, and no correction will be made for this except to consider it as a possible systematic error.

IV. MATRIX ELEMENTS AND THE SLOPES OF THE TRANSITION FREQUENCIES

A. Alkalis

In descriptions of χ'' such as Eq. (3), the μ_{ij} matrix dipole moment is an important quantity. If we take the rf field along the x direction it is given by $g\mu_B \langle i | S_x | j \rangle$. We have neglected the nuclear magnetic moment since it is about 10^{-3} smaller than that of the electron. In this experiment, transitions involving a change in the orientation of the nuclear magnetic dipole as well as that of the electron always had intensities less than 10% of those involving only a reorientation of the electronic magnetic dipole. Since the relative intensity was measured, all constants such as $g\mu_B$ cancel out, and one needs only to determine $\langle i | S_x | j \rangle$. (A quantity proportional to the matrix element, $\gamma = 2\mu_{ij}/h$, will be used later. It should be kept in mind that this quantity is not equal to the slope of the transition frequency, except at high fields.) Because the field is varied rather

¹² F. Bloch, Phys. Rev. **70**, 460 (1946).

¹³ D. M. S. Bagguley and J. H. E. Griffiths, Proc. Roy. Soc. (London) **A201**, 366 (1950).

¹⁴ K. Kumagai, K. Ono, I. Hayashi, H. Abe, J. Shimada, H. Shono, H. Ibamoto, and S. Tachimori, J. Phys. Soc. Japan **9**, 369 (1954).

TABLE I. Relative strengths and slopes of the alkali transitions.

Transition	Field (Gauss)	$\langle i S_x j\rangle^2$	$\partial\omega/\partial H$
Rb ⁸⁵ $m_F = -1, m_I = -\frac{1}{2}$ to $m_F = 0, m_I = -\frac{1}{2}$	4100	1/4	$g\mu_B/h$
Rb ⁸⁷ $m_F = -1, m_I = -\frac{1}{2}$ to $m_F = 0, m_I = -\frac{1}{2}$	2900	0.711/4	$0.686g\mu_B/h$
Cs ¹³³ $m_F = -3, m_I = -\frac{5}{2}$ to $m_F = -2, m_I = -\frac{5}{2}$	4100	0.658/4	$0.625g\mu_B/h$

than the frequency, the slope of the transition frequency, $\partial\omega/\partial H$, was also computed in order to convert the measurements from G to rad/sec.

In order to calculate $\langle i|S_x|j\rangle$ for an alkali atom, it is necessary to consider the Hamiltonian

$$\mathcal{H} = (g_N I_z + g_S S_z)\mu_B H_z + A \mathbf{I} \cdot \mathbf{S},$$

where g_N and g_S are the respective g values of the nucleus and electron in terms of the Bohr magneton, μ_B , I , and S are the angular momentum operators of the nucleus and electron, A is the hyperfine coupling constant, and H_z is the dc magnetic field. This Hamiltonian has energy eigenvalues given by the well-known Breit-Rabi formula.¹⁵ The wave functions in intermediate field will be linear combinations of the high-field wave functions which are eigenfunctions of I^2 , S^2 , I_z , S_z , and $F_z = I_z + S_z$. This energy is intermediate with respect to the hyperfine structure, and the reader is referred to the work of Condon and Shortley¹⁶ for a description of the eigenfunction and eigenvalue calculation. Using the experimental data in Ref. 15 and the energy levels computed from the Breit-Rabi formula, the matrix elements are computed in a straightforward manner. Likewise, the slope of the transition frequency is calculated by evaluating derivatives of the Breit-Rabi formula for the two levels of interest. The matrix elements of S_x and the slopes of the transitions used in determining the cross sections of the alkalis are shown in Table I. In the case of Rb⁸⁵, the field was sufficiently high in comparison to the hyperfine splitting, that one could just set $\gamma = \partial\omega/\partial H$.

B. Copper Sulfate

In the case of the $\text{CuSO}_4 \cdot 5\text{H}_2\text{O}$ crystal, the problem is more subtle. We will state only experimental and theoretical results and the reader is referred to the literature^{13,17} for further details.

The lowest state of a free Cu^{++} ion is a 2D state corresponding to an occupied $3d$ shell minus one electron. The effect of the crystalline field is to split the fivefold degenerate orbital state.

The wave functions do not depend on the magnetic field. The next highest energy level is approximately 1200 cm^{-1} away, and thus the two ground-state levels split linearly with the magnetic field. This was shown experimentally¹³ at wavelengths of 3.04 to 0.85 cm. Moreover, from Kramers theorem, one knows that the two levels are not split at zero magnetic field by the electric field. The slope of the transition frequency, therefore, is the ratio of the transition frequency to the transition magnetic field and is a constant.

It then follows that the g value at a given orientation will be proportional to the component of the magnetic dipole matrix element, $\mu_B(L + g_S S)$, along that direction. If one measures the g value of the transition with the dc magnetic field along the z axis of the crystal, one will have a measure of $\partial\omega/\partial H$. If one now rotates the crystal so that the field is perpendicular to the z axis and measures the g value at this orientation, one will have a measure of the matrix element giving the strength of the transition when the dc magnetic field is along the z axis. What one has done is to measure the off-diagonal matrix elements which give the strength of the transition by measuring the energy splitting caused by a dc field along the same orientation. This will be correct to the degree that the energy levels are linear in the field. In the case where the dc field is along the z axis, $\partial\omega/\partial H = g_{11}\mu_B/h$ and $\gamma = g_{11}\mu_B/h$. A similar combination would exist for any other orientation also.

In a $\text{CuSO}_4 \cdot 5\text{H}_2\text{O}$ crystal there are two sites for the copper ion with two magnetic axes, which are almost 90° apart. The g value for the dc field perpendicular to the plane of these axes has been measured¹³ to be 2.09 ± 0.01 . In the plane of the axes, the g value varies from 2.23 to 2.28. The intensity standard used in this experiment consisted of weighed out crystals which were oriented to give a g value of 2.08 ± 0.01 along the dc field. The rf field which is perpendicular to the dc field is in the plane of the two ion axes. In the calculations of the densities from the data, the value of the matrix element was taken to be $\gamma = (2.25 \pm 0.03)\mu_B/h$. The error includes all possible variations in the plane.

Finally, it should be pointed out that the absolute intensity has been measured¹⁸ and found to be within 5% of the results predicted from the dc susceptibility data. (However, no estimate of the limits of experimental error were given for this experiment.) Moreover, the paramagnetic-resonance g values¹³ agree closely with those predicted from the dc susceptibility data. To the best of our knowledge, then, the signals from the Cu^{++} ion are well understood, and all of the ions are contributing to the signal.

V. EXPERIMENTAL METHOD

For details of the method, the reader is referred to Ref. 26. A block diagram of the spectrometer is shown

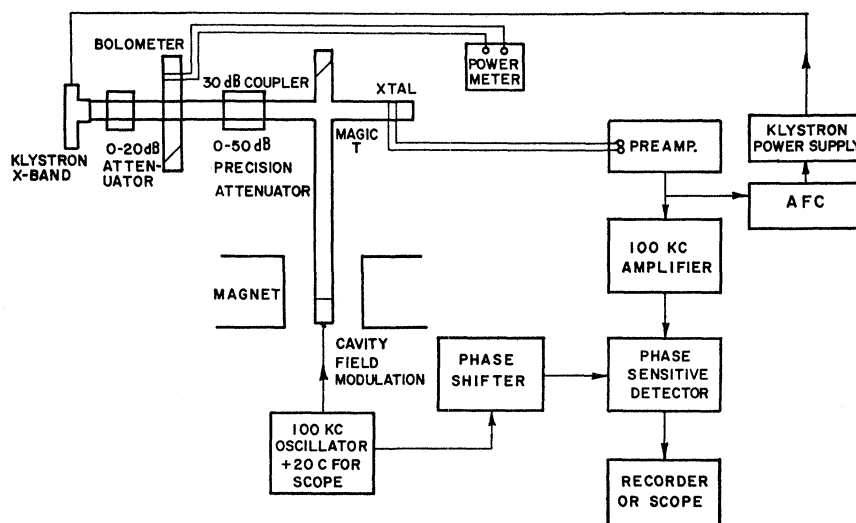
¹⁵ H. Kopfermann, *Nuclear Moments* (Academic Press Inc., New York, 1958), pp. 26 and 73.

¹⁶ E. U. Condon, and G. H. Shortley, *The Theory of Atomic Spectra* (Cambridge University Press, London, 1953), p. 152.

¹⁷ D. Polder, *Physica* **9**, 709 (1942). See also C. Kikuchi and R. D. Spence, *Am. J. Phys.* **18**, 167 (1950).

¹⁸ K. Kumagai, I. Hayashi, K. Ono, H. Abe, J. Shimada, and H. Shono, *J. Phys. Soc. Japan* **9**, 376 (1954).

FIG. 2. Block diagram of the equipment.



in Fig. 2. It is a standard x-band instrument with 100-kc/sec modulation of the magnetic field and phase-sensitive detection. The crystal bias current is caused by the mismatch of the cavity, and if the current is kept constant, the spectrometer will be a voltage detector, i.e., the signal displayed on the recorder will be proportional to the square root of the incident power. In the case of an unsaturated line, the displayed signal is

$$S \propto V_0 Q_L \eta (\partial \chi'' / \partial H) H_{M_{\text{eff}}}, \quad (4)$$

where V_0 is the square root of the incident power, Q_L is the loaded Q of the cavity, the filling factor is

$$\eta = \int_{\text{sample}} H_1^2 dV / \int_{\text{cavity}} H_1^2 dV, \quad (5)$$

the effective modulation is

$$H_{M_{\text{eff}}} = \int_{\text{sample}} H_M H_1^2 dV / \int_{\text{sample}} H_1^2 dV, \quad (6)$$

and $\partial \chi'' / \partial H$ is the derivative of the absorptive part of the susceptibility with respect to the magnetic field. The spectrometer was examined over the incident power range used and found to be a linear voltage detector within a few percent.

Taking a second derivative of Eq. (3), the maximum and minimum signals are found to occur at a separation (which we shall often refer to as the linewidth) of

$$\Delta H = \frac{2}{\sqrt{3}} \frac{1}{T_2 \partial \omega / \partial H}. \quad (7)$$

Calling the peak-to-peak voltage difference on the recorder ΔV , one obtains

$$\Delta V = \frac{A \gamma^2 \eta N H_{M_{\text{eff}}}}{T(2I+1)(2S+1)} \frac{1}{(\partial \omega / \partial H) (\Delta H)^2}, \quad (8)$$

where A is a single constant of proportionality incorporating the incident power, cavity Q , amplifier gain, etc.; A was either the same, or the ratio known in the comparison of the alkali signal with the copper sulfate signal in order to determine the density.

It is no problem to measure the linewidth and hence from Eq. (7), the effective lifetime T_2 . Then, once having determined the various constants in Eq. (8), the density N can be determined. In this experiment, crystals of copper sulfate were used as an intensity

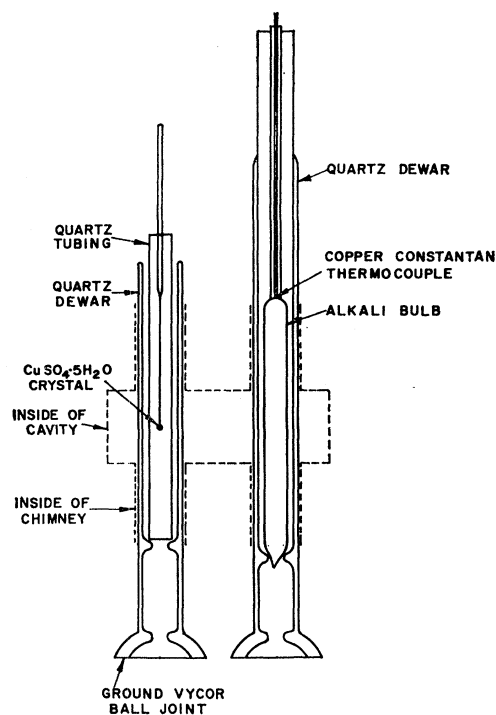


FIG. 3. Arrangement of Dewars and samples in the cavity (not to scale).

standard. Although there are two inequivalent Cu^{++} sites per unit cell, the strong exchange interaction smears these two lines together in one Lorentzian shape,^{13,14} so that the number of states, $(2I+1) \times (2S+1) = 2$.

Experimentally,¹⁹ the alkali sample and $\text{CuSO}_4 \cdot 5\text{H}_2\text{O}$ crystal were placed in a two-wavelength cavity as shown in Fig. 3. The cavity²⁰ was made out of Lava (American Lava Corporation) and painted on the inside with several coats of a silver glaze (Hanovia No. 32A silver paste). The alkali bulb was heated by passing warm nitrogen over it. A piece of quartz similar to that of the alkali bulb was placed in the copper sulfate Dewar so that the rf fields would be the same at both samples. The copper sulfate sample, glued on a thin, drawn-out filament of Pyrex tubing, was positioned in the maximum rf field.

The variation of the modulation amplitude along the Dewar was mapped. To determine the filling factor, the rf field intensity in the Dewars was probed by a DPPH (diphenyl picryl hydrazil) sample mounted on a very thin filament of Pyrex glass. When the signal is corrected for the variation of the modulation, a set of points which fall close to a $\cos^2 kx$ curve with half-wavelength of 2.9 cm was obtained. This is somewhat larger than the cavity width of 2.4 cm due to the fringing fields in the chimneys. The fringing fields in the chimneys were examined outside of the 2.9 cm and found to be negligible in the determination of the cross sections. The variation of the field intensity across the diameter of the bulb was measured to be certainly less than 9%. A comparison of the signal from the same DPPH sample placed in the copper sulfate Dewar and the alkali Dewar with two very similar pieces of quartz in position showed that

$$\frac{\Delta V_{\text{DPPH}}(\text{alkali position})}{\Delta V_{\text{DPPH}}(\text{CuSO}_4 \text{ position})} = 1.26 \pm 0.09. \quad (9)$$

An examination of the relative modulation amplitudes showed that almost all of the difference was due to this.

The ratios of $H_{M_{\text{eff}}}$ and η for the copper sulfate and the alkali samples were determined using Eqs. (6) and (5). $\cos^2(\pi x/2.7)$ was used as the distribution $H_M H_1^2$, and $\cos^2(\pi x/2.9)$ was used as the distribution of H_1^2 along the sample. Since the copper sulfate sample was quite small, only the peak modulation and rf fields are present and these are constant across the small sample. Therefore,

$$\frac{H_{M_{\text{eff}}}(\text{alk})}{H_M(\text{alk})} \frac{H_M(\text{CuSO}_4)}{H_{M_{\text{eff}}}(\text{CuSO}_4)} = 0.93 \pm 0.07. \quad (10)$$

The 7% error flag is an extreme value beyond which we do not expect the true value to lie. It is primarily

¹⁹ For a similar experimental arrangement, see D. Conrad, Z. Physik **162**, 160 (1961).

²⁰ J. Lambe and R. Ager, Rev. Sci. Instr. **30**, 599 (1959).

due to inexactness of the fit of the curve and deviations of the rf field from $\cos^2 kx$ near the chimneys. The ratio of $H_{M_{\text{eff}}}$ does not include the difference in signal due to different peak values of the modulation at the two samples. [See Eq. (9).]

The ratio of the filling factors is

$$\eta_{\text{Cu}}/\eta_{\text{A}} = v_{\text{Cu}}/\frac{1}{2}v_{\text{A}}, \quad (11)$$

where v_{A} is the volume of the alkali sample and v_{Cu} , the volume of the copper sulfate sample.

We are now able to determine the number of alkali atoms per cc, N_{A} , by taking the ratio of alkali signal to the $\text{CuSO}_4 \cdot 5\text{H}_2\text{O}$ signal. From Eq. (3), we have the number of alkali atoms per cc:

$$N_{\text{A}} = \frac{\mathfrak{N}_{\text{Cu}} \Delta V_{\text{A}} \Delta H_{\text{A}}^2 T_{\text{A}} (2I+1) \gamma_{\text{Cu}}^2 (\partial\omega/\partial H)_{\text{A}}}{v_{\text{A}} \Delta V_{\text{Cu}} \Delta H_{\text{Cu}}^2 \gamma_{\text{A}}^2 (\partial\omega/\partial H)_{\text{Cu}} (0.59)}. \quad (12)$$

$\mathfrak{N}_{\text{Cu}} = N_{\text{Cu}} v_{\text{Cu}}$ is the total number of Cu^{++} ions, and $0.59 = \frac{1}{2} \times 1.26 \times 0.93$ is the product of the numerical factors in Eqs. (9), (10), and (11).

The alkali bulbs were filled by sealing the $\frac{3}{16}$ -in. i.d. precision-bore quartz bulbs to a vacuum system in which the chloride of the alkali could be reacted with calcium hydride. The metal was then moved with a gas torch into the bulb. Typically, the pressure in the vacuum system when the bulb was pinched off was 10^{-4} mm of mercury.²¹

The samples were placed in the cavity as shown in Fig. 3. The alkali sample was then heated by passing nitrogen through an oven and up through the Dewar. The temperature was measured by a copper-Constantan thermocouple, calibrated against a thermometer, which was placed in a quartz tube attached to the sample as shown.

VI. DENSITY, LINEWIDTH, AND CROSS SECTIONS

The isotope Rb^{85} with a spin of $\frac{5}{2}$ and zero-field splitting of 3036 Mc/sec was studied somewhat more than the others. Because of the small hyperfine structure relative to the cavity frequency of 9000 Mc/sec, it is described quite well by the high-field approximation. The transitions obey the selection rule, $\Delta m_s = +1$, $\Delta m_l = 0$. Moreover, a calculation of the value of $\partial\omega/\partial H$, the slope of the transition frequency, for the six transitions gives values from $1.80 \mu_B/h$ for the lowest field line at 2300 G to $1.97 \mu_B/h$ for the highest at 4080 G. Thus, we see that the rate of change of the transition frequency was very close to the high-field case of $2.0 \mu_B$. The line at 4080 G was used in the determination of the cross section, and the values of γ and $\partial\omega/\partial H$ used were the high-field values. Study of the linewidths and signal heights for all of the lines showed that the linewidth in megacycles and signal height were the

²¹ It has been shown recently by T. Stark of this laboratory that the tipoff may introduce as much as 10^{-2} mm of foreign gases into the bulb. These gases could be responsible for much of the thermal relaxation measured and discussed in Sec. IX.

same to within $\pm 6\%$ for all of the lines. These results indicated a simple physical model for the gas which is valid in the high-field approximation, at least. The line-broadening mechanism is the same for all of the levels, and the spin-exchange-collision cross section for an atom is independent of which of the $2(2I+1)$ states it is in, to the accuracy of the experiment. Therefore, it was necessary to measure the cross section for only one transition.

Cs¹³³, with a spin of $\frac{7}{2}$ and hyperfine splitting of 9193 Mc/sec, had a considerably more complicated spectrum, giving lines from very low fields up to about 5900 G. The low-field selection rules, $\Delta F = \pm 1, 0$; $\Delta M_F = \pm 1$ applied. The highest field line is the only $\Delta F = 0$ line. The $\Delta F = 1, \Delta M_F = +1$ transition goes over into the high-field case of $\Delta M_s = +1, \Delta M_I = 0$, whereas the $\Delta F = 1, \Delta M_F = -1$ transition, which corresponds to $\Delta M_s = +1, \Delta M_I = -2$, dies out as the field at which the transition takes place grows large. However, because of the large hyperfine splitting, the $\Delta F = 1, \Delta M_F = -1$ transitions could be observed in all cases except the $(F=3, M_F = -2) - (4, -3)$ case at 4100 G. Moreover, an examination of the Breit-Rabi formula shows that "mirror" transitions [e.g., $(3, -1) - (4, -2)$ and $(3, -2) - (4, -1)$] lie almost on top of each other, split only by a difference on the order of $\mu_N H$, where μ_N is the nuclear magnetic moment. In order to study these transitions it would have been necessary to use only very narrow lines, which introduces considerable error, and to correct for the superposition of one part of the doublet upon the other. Thus, there were only two transitions, the $(3, -3) - (4, -2)$ transition at 4100 G and the $(4, -4) - (4, -3)$ transition at 5900 G (this is a $\Delta F = 0$ transition), which were usable. Because our magnet was not designed for prolonged use at fields on the order of 5900 G, only the $(3, -3) - (4, -2)$ transition was convenient to study. A comparison of the width of the $(3, -3) - (4, -2)$ transition and the widths of the doublet $(3, -2) - (4, -1)$ and $(3, -1) - (4, -2)$ showed that the linewidths in frequency units were the same. Because of this and the results of our rather intensive study of Rb⁸⁵, which gave such a simple model of the collision processes, only the above-mentioned transition was used in the determination of the cross section.⁹

Rb⁸⁷ has a spin of $\frac{3}{2}$ and hyperfine splitting of 6835 Mc/sec. The $(1, -1) - (2, 0)$ transition at 2900 G was used. A calculation of the transition at 2900 G was used. A calculation of the transition probabilities showed that the strength of the mirror transition, $(1, 0) - (2, -1)$ was less than 10% of the $(1, -1) - (2, 0)$ transition. Since the lines are split by several gauss, we expect no significant error to be caused by the smaller line.

Having measured all of the various quantities mentioned in Sec. V, N_a could then be computed and the variation of linewidth with density could be studied. Typical plots are shown in Fig. 4. The linewidth varies

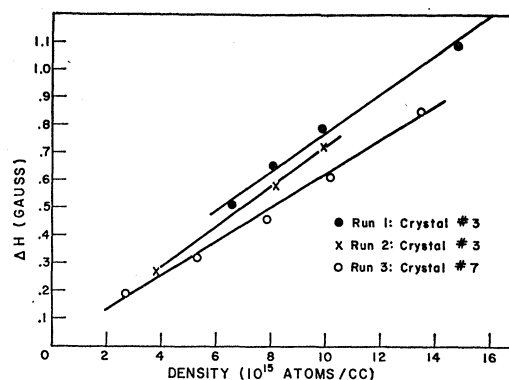


FIG. 4. Results of three typical runs on Rb⁸⁵.

linearly with the density. This agrees with the ideas about a linewidth caused by spin-exchange collisions. The data shown in Fig. 4 consists of three different runs. Crystal 3 was an unoriented crystal which was standardized by comparing with three weighed, oriented crystals. This was done with an experimental standard deviation error of $\pm 11\%$. Crystal 7 was one of these weighed out, oriented crystals. The primary error does not seem to lie in a given run, but in variations from run to run. The results on Cs¹³³ and Rb⁸⁷ gave straight-line plots and confirmed the model employed for Rb⁸⁵. The results on Rb⁸⁵ involve a wider range of experimental conditions and gave a somewhat better idea of the experimental errors involved.

In Table II we have listed the results of all of the runs. Since the runs with crystal 3 contained two errors, namely the random error in the slope of $\pm 10\%$ and the random error in the calibration of the crystal of $\pm 11\%$, the averages were weighted according to the error, with a $\pm 15\%$ error assigned to the runs with crystal 3 and $\pm 10\%$ error assigned to the other runs. This error does not include systematic errors inherent to all the runs. (See Sec. VII.) In addition to the rate of change of linewidth with density, $\delta\Delta H/\delta N$, the rate of change of the half-width at half-power with density

TABLE II. Rate of change of linewidth with density.

Atom	Slope: $\delta\Delta H/\delta N$ G/10 ¹⁶ atoms	Average slope G/10 ¹⁶ atoms	$\delta\Delta f_{1/2}/\delta N$ Mc/sec/10 ¹⁶ atoms
Rb ^{85a}	0.71	0.68	1.6
	0.72		
	0.61		
	0.67		
	0.72		
Rb ⁸⁷	1.13	0.98	1.5
	0.92		
	0.90		
Cs ¹³³	1.01	0.92	1.4
	0.94		
	0.85		

^a In taking the averages, the first two runs on Rb⁸⁵ and the first one on Rb⁸⁷ and Cs¹³³ were given a weight of 0.44 = $(10\%/15\%)^2$. See Sec. VII for an estimation of the error of this experiment.

TABLE III. Measured spin-dephasing cross sections of Rb⁸⁵, Rb⁸⁷, and Cs¹³³.

Atom	
Rb ^{85a}	$(2.0 \pm 0.4) \times 10^{-14}$ cm ²
Rb ⁸⁷	$(1.9 \pm 0.4) \times 10^{-14}$ cm ²
Cs ¹³³	$(2.3 \pm 0.5) \times 10^{-14}$ cm ²

^a The assigned limits of error are discussed in Sec. VII.

in frequency units, $\Delta f_{1/2} = 1/2\pi T_2$, is tabulated. This quantity, which is more useful in applying the results to other experiments, is tabulated along with $\delta\Delta H/\delta N$ for the three alkali atoms studied.

It should be remembered in using this data that the temperature at which these measurements were taken was approximately 540°K. In a typical optical pumping experiment at almost half this temperature, the average velocity will be down by a factor of $1/\sqrt{2}$ and hence, the collision frequency per unit density, also. Purcell and Field¹ have shown that, in the case of atomic hydrogen, the cross section is a soft function of the temperature. The temperature range employed here is too small to show any variation in the rate of change of the collision frequency, even that due to the change in the average velocity.

The rate of change of the linewidth with density has been measured. However, in order to put the results in a form which is more meaningful on an atomic level, they are restated in terms of an effective spin dephasing collision cross section. The cross section will be calculated as if it were due to hard-sphere collisions,²² using Eq. (1).

In terms of the slopes of the straight lines plotted for each run, the equation for the dephasing cross section becomes

$$\sigma_{\text{deph.}} = \frac{1}{2} \left(\frac{3}{2}\right)^{1/2} \frac{\delta\Delta H}{\delta N_a} \frac{\partial\omega/\partial H}{\bar{c}}, \quad (13)$$

where \bar{c} is the mean velocity and was computed at a temperature of 546°K. The cross sections are given in Table III.

The atoms in a collision must have different m_I values in order to affect the linewidth. The measured cross section should be corrected by $(2I+1)/2I$ [see Eq. (2)]. For Rb⁸⁵, $I = \frac{5}{2}$ and Rb⁸⁷, $I = \frac{3}{2}$, we have correction factors of 6/5 and 4/3. This is a difference of ± 0.07 about an average value of 1.27. Our measurements were not precise enough to detect such a small difference. *The values in Table III are not corrected by these factors.*

VII. ESTIMATION OF THE ERROR

A. Random Errors

The random errors came from a large number of sources. The limited signal-to-noise ratio in the meas-

²² J. Jeans, *An Introduction to the Kinetic Theory of Gases* (Cambridge University Press, London, 1952), p. 135.

TABLE IV. 70% probable errors in determination of the cross section.

Source	Size
Random	$\pm 10\%$
Variation of quartz tubing	$\pm 5\%$
Effect of films	-7%
Alkali field sweep	$\pm 2\%$
Copper sulfate field	$\pm 4\%$
Temperature of alkali	$\pm 1\%$
Temperature of copper sulfate	$\left\{ \begin{array}{l} +3\% \\ -1\% \end{array} \right.$
Determination of ratio of signals in both Dewars	$\pm 5\%$
Determination of volume	$\pm 5\%$
Determination of $H_{M,eff}$	$\pm 5\%$
Copper sulfate line shape	-10%
$\gamma_{Cu^{2+}}$ and $\partial\omega/\partial H _{Cu}$	$\pm 4\%$
Miscellaneous	$\pm 5\%$

urement of the linewidth and signal height contributed heavily to the small deviations about each line. There were also many other factors, such as small temperature changes during a measurement. However, variation of the slopes rather than the points about the line was the chief source of random error. This was caused by errors which were systematic for a given run, such as the inexact positioning of the copper sulfate sample. The presence of metallic films and droplets in the bulbs during the experiment also contributed. This will be discussed further in the section on systematic error. The 70% probable random error is taken to be $\pm 10\%$.

B. Systematic Errors

In this experiment systematic errors, which do not display themselves with the same facility as random errors, are a large source of inaccuracy. Let us first deal with errors that have to do with the measurements and the apparatus and then go on and discuss certain physical assumptions which have been made, such as the shape of the line. The results are summarized in Table IV. The method employed has been to estimate the extreme error limit of an effect and then take 0.7 of this value as the 70% probable error. The errors listed in Table IV are the 70% probable errors. The sign indicates the change in the cross section if the error exists.

The experiment involves putting a quartz bulb containing an alkali metal into a microwave cavity. Both the quartz and the metal affect the microwave fields in the cavity. The bulb was placed in a region of minimal electric field. However, small variations in the size of each quartz tube might cause a change in the rf magnetic field intensity in the bulb. The signals from a DPPH sample inside four different tubes of standard inside diameter but with outside diameter ranging from 0.270 to 0.284 in. were compared. After correcting for the change in Q (monitored by a copper sulfate sample) it was found that the extreme deviation among the quartz tubes was $\pm 3\%$, with no pattern of increase or

decrease indicated. The tubes used in calibration and the bulbs ranged in outside diameter from 0.269 to 0.276 in., a range only half as wide as the one studied. Therefore, to within $\pm 7\%$ (the experimental error of this type of measurement) the rf field intensity does not change from one bulb or tube to the next.

The alkali metal formed films of metal on the inside of the bulb. A few very small droplets of metal, 1 mm or less in size, were present sometimes; but they were not observed to affect the microwave field significantly. Because of their extremely small size in comparison to the diameter of the bulb, their perturbation of the field was highly localized. If the film was thick enough to destroy the cavity resonance, the bulb was placed in an oven and aged. This reduced the film thickness by causing the alkali to react with the walls, forming a brownish layer on the inside.²³ The brown layer on the inside of the bulb had a low conductivity and did not perturb the microwave field. This was evidenced by two observations. First, the cavity Q_L improved as the bulb aged, approaching the value of 3000 obtained with ordinary quartz. Secondly, a bulb which had lost its signal due to aging was opened, and the signal from a DPPH sample placed inside was compared with the signal in a similar sized piece of quartz tubing. No difference was found. The alkali metal film, however, very definitely lowered the Q of the cavity. The primary question was whether it was acting only as an extremely thin but very (due to its high conductivity) lossy film, or whether it was perturbing the configuration of the field and partially shielding the gas from the microwave magnetic field. Using Slater's perturbation theorem,²⁴ one sees that for a region of high microwave magnetic field the shift of the resonant frequency caused by removal of part of the volume is approximately the excluded volume divided by the cavity volume times the resonant frequency. Assuming 20% shielding of the sample bulb, a shift of +40 Mc/sec is calculated. The Q of the cavity was changed over a factor of four by raising the temperature of a bulb. The total frequency shift was less than two Mc/sec. Because the sample was heated and not the cavity as a whole, the cavity was very stable with respect to frequency changes. Frequency shifts as large as 40 Mc/sec, were never observed while making the measurements on the cross sections.

There is other evidence. From the results, the line-width, ΔH , is a constant times the alkali density, N_a . From Eq. (8), the product $\Delta H \cdot \Delta V$ is a constant for a given line, depending only on the Q , modulation in-

tensity, and amplifier gain, but not on the width of the line. The signal from a given line of two Cs¹³³ bulbs was compared. The Q of these two bulbs differed by two or more, depending on the temperature, because one bulb had more metal than the other. Three measurements were made at different temperatures on one bulb and two on the other. When corrected for differences in Q , amplifier gain, and modulation intensity, it was found that all of the products $\Delta V \Delta H$ agreed to within $\pm 12\%$. This is good agreement when one considers the extreme range of conditions involved and the errors of measurement.

On the basis of this evidence, it was concluded that the effect of the alkali films was primarily to lower the Q without perturbing the field. Because of the high Q of the bulbs used and the fact that no appreciable changes in frequency with temperature were observed, we conclude that any shielding of the field was less than 10%. This is understandable because the films were so extremely thin in comparison to a skin depth that the configuration of the microwave field did not change its configuration but dissipated itself in the high conductivity film, lowering the Q .

The field sweep was calibrated with a random error of about 1%. A motor driven Helipot was used to provide a changing reference voltage to the electromagnet. The same part of the Helipot (the center) on the sweep was always used in taking data. The field sweep was found to be slightly nonlinear, but the error caused by this is estimated to be less than 1%. Checks of the sweep at 4000 G four and seven months later showed agreement to within 3%. The extreme deviation of the sweep was taken as $\pm 3\%$.

The calibration of the thermocouple may have been off by several degrees. This is a very small error. However, the part of the bulb in the cavity may have been hotter than the part touching the thermocouple. Comparison of one of the runs on a fresh Rb⁸⁵ bulb showed that the data at each temperature was within 15% of that given by Dushman.²⁵ From the lifetime of the bulbs (10 to 100 h) one can estimate the rate at which the walls are removing the alkali. A simple steady-state calculation using 0.02 cm² as the effective area of the emitting film shows that the pressure in the bulb should be that of thermal equilibrium within a part in a thousand. (This is not true at optical pumping temperature where evaporation rates are 10⁵ lower.) If there were a significant difference between the thermocouple temperature and the actual temperature, there would be a large discrepancy between these densities and Dushman's. From his data, it is seen that a 5% difference of 25° would imply a discrepancy of a factor of two. Because of the previously mentioned calculation, the rate at which the walls of the bulb are removing alkali does not affect the pressure

²³ The brownish layer was probably due to some type of damage center caused by the alkali. A short search for paramagnetic resonance lines was made with one of the bulbs at liquid nitrogen temperatures, but no lines were found. When a bulb in which all of the metal was used up was opened to air, the brownish layer disappeared overnight leaving a whitish deposit such as that left when thin alkali metal films react with air. This deposit, however, did not dissolve in dilute hydrochloric acid.

²⁴ J. C. Slater, Rev. Mod. Phys. 18, 482 (1946).

²⁵ S. Dushman, *Scientific Foundations of Vacuum Technique* (John Wiley & Sons, Inc., New York, 1949), p. 746.

in the bulb by this large an amount and the measured density is close to that of thermal equilibrium. Therefore, since the measured densities are so close, it may be concluded that the thermocouple temperature was quite close to the true temperature. The extremes of error are taken as +2% and -1%. This is also evidence of thermal equilibrium in the bulb.

The copper sulfate temperature was measured at the end of a run by placing a thermometer in the copper sulfate Dewar. Since the thermometer gives a slightly different impedance to the cooling gas flow than the sample and quartz tube, the temperature given by a thermometer was checked by interchanging with a thermocouple in a quartz tube near a copper sulfate sample. The thermometer was found to read 5 to 10° below the thermocouple. An extreme of error was assigned to the temperature as determined by the thermometer of +4% and -2%.

The ratio of the signal in the standard position to the signal in the alkali position was determined [see Eq. (9)] with an error of no more than ±7%. The volume of the alkali bulb and $H_{M_{eff}}$ had similar errors in their determination.

One must now discuss some of the physical assumptions made in this measurement. These are connected directly with the previous discussion of Secs. III and IV on line shapes and matrix elements. It was assumed that the lines studied were Lorentzian, and it was shown that this was true within experimental error. However, because of the comparatively large contribution from the tails of a Lorentzian line, deviations far out will give significant errors. In the case of the alkali signals, there are good reasons for expecting the line to be Lorentzian (see Sec. III).

The determination of the line shape in copper sulfate is a somewhat more acute problem. It was used as an absolute intensity standard in order to determine the number of alkali atoms in the bulb. If it varies from the assumed intensity, the calculated number of alkali atoms and hence cross sections will be inaccurate. In Sec. III it was shown that the deviation of the line from a Lorentzian shape would contribute an error of less than 20%. If the line were Lorentzian out to one more linewidth, this would be reduced to about 10%. Because of the very good agreement of the line with a Lorentzian shape and the fact that the line does not drop to zero at the assumed cutoff point—which was the extreme assumption which was made—it is felt that 10% is a more realistic estimate of the 70% probable error caused by the line shape.

The possible extreme deviations of γ_{Cu} and $\partial\omega/\partial H_{Cu}$ were evaluated. Allowing for a possible 10° tilt of the crystal, the extreme deviation of the quantity $[\gamma_{Cu}^2/(\partial\omega/\partial H)]_{Cu}$ is ±5%.

There were also several small sources of error such as small nonlinearities in the spectrometer, the amplifier, and the recorder. All of these errors were certainly less than ±7%. Since the errors are independent, the

square root of the sum of the squares was taken in Table IV in order to find a 70% probable error of ±20%.

VIII. THERMAL RELAXATION TIME

In order to verify that the cross sections were due to spin exchange, and not to some other *thermal* relaxation mechanism, the thermal relaxation time T_1 was measured by a saturation of the signal. In exchange collisions the spin angular momentum is conserved, and in high field where the energy depends on the spin angular momentum one does not expect the exchange collisions to be a relaxation mechanism.

As mentioned previously, the rf magnetic field distribution was constant across the diameter of the sample bulb, but varied as $\cos^2 kx$ along the length, peaking at the center and going nearly to zero when the bulb was no longer in the cavity. Hence, in a saturation experiment the saturation term $\gamma^2 H_1^2 T_1 T_2 = A$ was not a constant, but varied along the length of the sample. In order to relate this term to the ratios of the signal measured, the signal from the volume element of length dx was calculated and the result then integrated along the length of the bulb.²⁶ In using this method, the same characteristic thermal relaxation time was assumed for all parts of the bulb.

Let case 1 be when A is much less than one and can be set equal to zero. Case 2 is at a higher power where A cannot be neglected and saturation of the signal exists. Taking the ratio of the signals at the derivative extrema, we obtained for these Lorentzian lines

$$\Delta V_1 V_2 / \Delta V_2 V_1 = \frac{1}{2} \left[\left(1 + \frac{3}{4} A \right)^{1/2} + 1 \right]^2 \times \left[\left(1 + \frac{3}{4} A \right)^{1/2} - \frac{1}{2} \right], \quad (14)$$

where ΔV_1 and ΔV_2 are the measured recorder displacements at the derivative extrema. V_2/V_1 is simply the square root of the ratios of the incident power. In order to relate $(\Delta V_1/\Delta V_2)(V_2/V_1)$ to the quantity of interest, $A = \gamma^2 H_1^2 T_1 T_2$, a plot was made of this ratio over a wide range of values of A . Using the measured ratio, $(\Delta V_1/\Delta V_2)(V_2/V_1)$, the value of A could be read from the graph.

The thermal relaxation time was measured by a procedure similar to that used in measuring the cross sections. After the temperature of the bulb came to steady state, the signal was recorded at two very different powers. The power was always low enough for A to be taken as zero. A piece of DPPH was placed in the copper sulfate Dewar. The signal from this sample was proportional to the Q of the cavity which changed as a function of bulb temperature due to changes in the films in the bulb and the temperature of the cavity. After all of the measurements were completed, the system was allowed to cool to room

²⁶ Details of this calculation may be found in the thesis of H. W. Moos, University of Michigan, 1961 (unpublished), University Microfilms, Inc., Ann Arbor, Michigan.

temperature and the DPPH signal recorded there also. The maximum rf magnetic field intensity was then measured by saturating a sample of known T_1 . Working backwards, H_1^2 was then determined at a given incident power. Crystalline free radicals have narrow Lorentzian lines at $g=2.0$, caused by exchange, with the property that $T_1=T_2$.²⁷ Thus, the thermal relaxation time can be measured by simply measuring the width of the line. A small sample of α , γ -bisdiphenylene- β -phenylallyl²⁸ placed in the maximum rf field and rotated for minimum linewidth was used.

Rb⁸⁵ was studied most thoroughly. A study of all the lines at one temperature and power showed that the saturation term A varied from 2.1 at high field to 1.8 at low field. This is a difference of only 15% and was within the errors of the measurement. To within the errors of the measurement, the thermal relaxation time, T_1 , is the same for all of the lines. The results for the highest field line, $m_I = -\frac{5}{2}$ of Rb⁸⁵ are shown in Fig. 5, where the linewidth ΔH is plotted against the measured $1/T_1$. A similar, but not identical, set of results was found for the $F=2$, $m_F = -1$ to $F=3$, $m_F=0$ transition of Rb⁸⁷. The errors in the determination of T_1 are primarily systematic such as an uncertainty in H_1^2 of $\pm 20\%$ and are estimated to be about $\pm 30\%$.

The relaxation time of Cs¹³³ was examined by saturation, also, but with not as high precision. The results found were similar to those of Rb⁸⁵ and Rb⁸⁷; T_1 does not equal T_2 .

IX. RELAXATION CROSS SECTION

The values of T_1 measured are sufficiently short to cause inquiry. The reason for this is best seen by noting that each pair of levels associated with a given nuclear orientation m_I is coupled to the other by spin-exchange collisions, and excess or deficiency of polarization is rapidly transferred from one pair of levels to another. Thus, while only one pair of levels is absorbing, all of

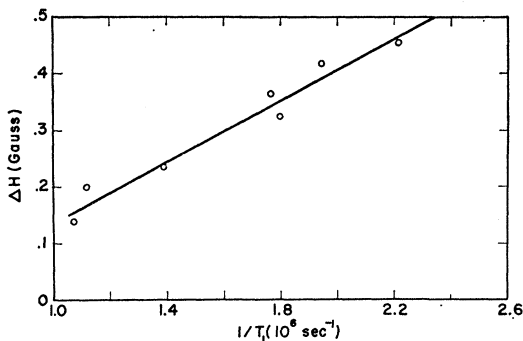


FIG. 5. Experimentally determined values of ΔH and $1/T_1$ for Rb⁸⁵.

²⁷ J. P. Goldsborough, M. Mandel, and G. E. Pake, Phys. Rev. Letters 4, 13 (1960).

²⁸ J. E. Wertz, Chem. Rev. 55, 829 (1955).

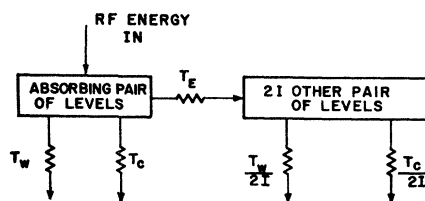


FIG. 6. Schematic representation of the relaxation paths and times.

the levels are removing energy from the spin system by thermalizing collisions with each other, impurities, and the wall. This shortens the measured T_1 by a considerable factor.

The results for Rb⁸⁵ and Rb⁸⁷ were analyzed further and a cross section for the thermal relaxation process estimated from the experimentally measured values of T_1 . The relaxation processes are represented schematically in Fig. 6.

The rf energy is absorbed by one pair of levels which relax directly at a rate $1/T_C + 1/T_W$, where $1/T_W$ is the collision rate with the wall and $1/T_C$ is the thermal relaxation rate due to atomic collisions. However, the excess energy is also transferred by spin-exchange collisions to the $2I$ other pairs of levels at a rate $1/T_E$. T_E is the spin polarization transfer time and is on the order of

$$1/T_E = 1/T_2 - 1/T_2^* - 1/T_W - 1/T_C, \quad (15)$$

where $1/T_2^*$ is due to the magnet inhomogeneity. These levels then relax at a total rate of

$$2I(1/T_W + 1/T_C). \quad (16)$$

Here one has neglected differences in T_C , population differences, and small variations in the cross section among the various pairs of levels. The relaxation rate is then given by

$$\frac{1}{T_1} = \frac{1}{T_W} + \frac{1}{T_C} + \frac{1}{T_E + (1/2I)(1/T_W + 1/T_C)^{-1}}. \quad (17)$$

Neglecting T_W and T_2^* in Eq. (17), we see that if $1/T_C$ starts to contribute appreciably to the linewidth, $1/T_2$, T_1 approaches T_2 very rapidly because of exchange which distributes the energy among the other pairs of levels, making the thermal relaxation mechanisms much more effective. Thus, the measurement of T_1 is a very effective way of detecting whether T_C will have an appreciable contribution to T_2 . Using the values from the straight-line plots such as in Fig. 5, $1/T_C$ was computed for Rb⁸⁵ and Rb⁸⁷. (To calculate the wall time T_W we calculated the rate of absorption of energy from the field, the rate at which it is removed by collisions with the wall and demanded that their rates be equal.) We compute, neglecting end effects, that for a cylinder of radius R ,

$$T_w = 2R/C$$

(for rubidium, $T_w = 13 \times 10^{-6}$ sec).

The data described in Sec. VI were then used to estimate the density of atoms at a given linewidth, and the thermal relaxation cross section for Rb⁸⁵ and Rb⁸⁷ was estimated to be on the order of 6×10^{-16} cm². The important point is that the thermal relaxation mechanisms do not appear to be contributing appreciably to the linewidth. The exact natures of these relaxation mechanisms are currently under investigation in this laboratory.

REMARKS ON SPIN-EXCHANGE CROSS SECTIONS

In view of the interest in the exchange cross section, the relation between the dephasing cross section for Rb⁸⁵-Rb⁸⁵ and the exchange cross section will be restated here. Unfortunately, there is confusion as to just how to define an exchange cross section; therefore, the cross section for an *observable transfer of electronic spin polarization* (180° phase change) will be used.

$$\sigma_{\text{exchange}} \equiv \sigma_{\text{polarization transfer}} = \frac{1}{4}\pi a^2 = \frac{1}{4}\sigma_{\text{coll}},$$

where a is the impact parameter for a collision with another atom in an *unlabeled spin state*. σ_{coll} is the same as in Ref. 10. Thus in the high-field limit,

$$\sigma_{\text{ex}} \equiv \sigma_{\text{pol trans}} = [(2I+1)/4I]\sigma_{\text{dephasing}}.$$

This relation yields

$$(\sigma_{\text{ex}})_{\text{Rb}^{85}-\text{Rb}^{85}} = (1.2 \pm 0.2) \times 10^{-14} \text{ cm}^2.$$

Using the same relation (not justified in this paper) for Rb⁸⁷,

$$(\sigma_{\text{ex}})_{\text{Rb}^{87}-\text{Rb}^{87}} = (1.3 \pm 0.2) \times 10^{-14} \text{ cm}^2.$$

These are to be compared with the measurement of S. M. Jarrett,²⁹ in which he measures a Q_x defined as the cross section for an observable transfer of polarization (180° phase change referred to the Z axis) between oppositely oriented spins (labeled before collision). For example, the rate at which a Rb⁸⁷ atom in the spin-down state makes transitions to the spin-up state is given by

$$n_+ Q_x \langle v \rangle_{\text{rms}} = \frac{1}{2} n Q_x \langle v \rangle_{\text{rms}} = n \sigma_{\text{ex}} \bar{v}_{\text{rel}},$$

²⁹ S. M. Jarrett, Phys. Rev. **133**, A111 (1964).

where σ_{ex} is as defined above, n is the number of Rb⁸⁵ atoms per unit volume, $\langle v \rangle_{\text{rms}}$ is the rms relative velocity which Jarrett calls \bar{v} , and \bar{v}_{rel} is the average relative velocity between atoms used in this paper. Thus

$$\sigma_{\text{ex}} = \frac{\langle v \rangle_{\text{rms}} Q_x}{\bar{v}_{\text{rel}} 2} = (0.96 \pm 0.11) \times 10^{-14} \text{ cm}^2$$

from Jarrett's measurement at the lower temperature ($\sim 360^\circ\text{K}$). These experiments are in excellent agreement and indicate only a very weak temperature dependence, if any, over this range. This is evidence that the spin exchange proceeds by single, large, phase collisions and adds credibility to the above relationship between the dephasing and exchange cross sections.

CONCLUSION

This paper has reported a paramagnetic resonance study of the Zeeman transitions in Rb⁸⁵, Rb⁸⁷, and Cs¹³³. Specifically, the linewidth as a function of density was examined. The results were stated in terms of a spin-dephasing cross section with an estimated 70% probable error of $\pm 20\%$. The measured dephasing cross sections for Rb⁸⁵, Rb⁸⁷, and Cs¹³³ were 2.0, 1.9, and 2.3×10^{-14} cm².

The thermal relaxation times of Rb⁸⁵, Rb⁸⁷, were measured. Due to the exchange mechanism which spread the absorbed rf energy to all of the atoms, the effective times were quite short. A cross section for thermal relaxation was computed from the data which indicated that thermal relaxation processes do not contribute appreciably to the linewidth. It is felt, however, that more precise and extended measurements of the thermal relaxation times of the alkalis are needed to pinpoint their cause.

ACKNOWLEDGMENTS

The authors wish to thank Professor Peter Franken for many stimulating conversations which helped to clarify our interpretations. The assistance of Joseph Horner in the latter stages of the experiment is gratefully acknowledged.